EPJ manuscript No.
(will be inserted by the editor)

SLAC-PUB-10208
CERN-TH/2003-249
PITHA 03/09
MCTP-03-46
hep-ph/0310187

New NNLL QCD Results on the Decay $B \to X_s \ell^+ \ell^{-\star}$

A. Ghinculov[1], T. Hurth[a 2], G. Isidori[3], and Y.-P. Yao[4]

[1] Department of Physics, University of Rochester, Rochester, NY 14627, USA
[2] Theoretical Physics Division, CERN, CH-1211 Genève 23, Switzerland and SLAC, Stanford University, Stanford, CA 94309, USA
[3] INFN, Laboratori Nazionali di Frascati, I-00044 Frascati, Italy
[4] Michigan Center for Theoretical Physics, Univ. of Michigan, Ann Arbor MI 48109-1120, USA

Abstract. We present here new NNLL predictions on the inclusive rare decay $B \to X_s \ell^+ \ell^-$ based on our new two-loop QCD analysis of the four-quark operators.

PACS. 12.38.Cy, 13.66.Jn, 13.20.He.

1 Introduction

The rare decay $B \to X_s \ell^+ \ell^-$ offers the B factories the possibility to open a new interesting window on flavour physics. A measurement of the dilepton spectrum and of the forward–backward asymmetry in this decay process has been proposed as a way to test for new physics and discriminating between different new physics scenarios (for a recent review see [1]). Indeed, the short-distance-dominated flavour-changing neutral-current amplitude of $B \to X_s \ell^+ \ell^-$ is extremely sensitive to possible new degrees of freedom, even if these appear well above the electroweak scale. This type of indirect search for new physics relies both on an accurate measurement of the dilepton spectrum, and on an accurate theoretical calculation of the decay probability. The inclusive $B \to X_s \ell^+ \ell^-$ transition just starts to be accessible at the B factories: BELLE and BABAR have already data on the rate based on a semi-inclusive analysis [2,3,4]. These first measurements are in agreement with SM expectations, but are still affected by a 30% error: substantial improvements can be expected in the near future.

From the theoretical point of view, inclusive rare decay modes like $B \to X_s \ell^+ \ell^-$ are very attractive because, in contrast to most of the exclusive channels, they are theoretically clean observables dominated by the partonic contributions. Non-perturbative effects in these transitions are small and can be systematically accounted for, through an expansion in inverse powers of the heavy b quark mass. In the specific case of $B \to X_s \ell^+ \ell^-$, the latter statement is applicable only if the $c\bar{c}$ resonances that show up as large peaks in the dilepton invariant mass spectrum (see fig. 1) are removed by appropriate kinematic cuts. In the *perturbative windows*, namely in the region below and in the one above the resonances, theoretical predictions for the invariant mass spectrum are dominated by the purely perturbative contributions, and a theoretical precision comparable with the one reached in the decay $B \to X_s \gamma$ is in principle possible [5,6]. Regarding the choice of precise cuts in the dilepton mass spectrum, it is important to stress that the maximal precision is obtained when theory and experiments are compared employing the same energy cuts and avoiding any kind of extrapolation.

In these processes QCD corrections lead to a sizable modification of the pure short-distance electroweak contribution, generating large logarithms of the form $\alpha_s^n(m_b) \times \log^m(m_b/M_{\rm heavy})$, where $M_{\rm heavy} = O(M_W)$ and $m \leq n$ (with $n = 0, 1, 2, ...$). These effects are induced by hard–gluon exchange between the quark lines of the one-loop electroweak diagrams. The most suitable framework for their necessary resummations is an effective low-energy theory with five quarks, obtained by integrating out the heavy degrees of freedom. Renormalization-group (RG) techniques allow for the resummation of the series of leading logarithms (LL), $\alpha_s^n(m_b)\ \log^n(m_b/M)$, next-to-leading logarithms (NLL), $\alpha_s^{n+1}(m_b)\ \log^n(m_b/M)$, and so on.

2 NNLL Calculation

For a detailed discussion of the present status of the perturbative contributions to decay rate and FB asymmetry of $B \to X_s \ell^+ \ell^-$ we refer to [1]. Here we simply recall that the complete NLL contributions to the decay amplitude can be found in [7]. Since the LL contribution to the rate turns out to be numerically rather small, NLL terms represent an $O(1)$ correction and a computation of

* Contribution to International Europhysics Conference on High Energy Physics EPS03, 17-23 July, Aachen, Germany, presented by T.H.

[a] Heisenberg Fellow

Work supported by the Department of Energy contract DE-AC03-76SF00515.
Stanford Linear Accelerator Center, Stanford University, Stanford, CA 94309

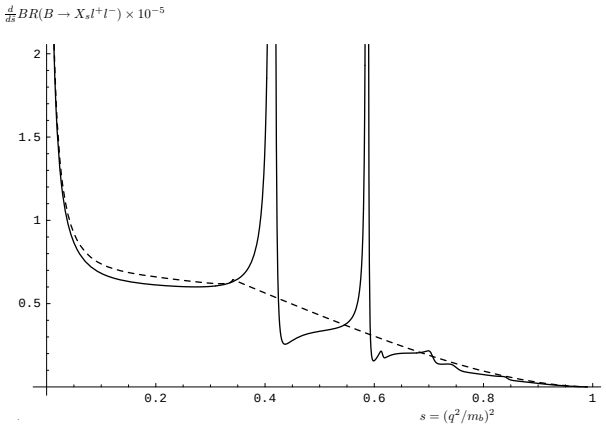

Fig. 1. Schematic dilepton mass spectrum of $B \to X_s \ell^+ \ell^-$, the dashed line corresponds to the perturbative contribution

NNLL terms is needed if we aim for a numerical accuracy below 10%, similar to the one achieved by the NLL calculation of $B \to X_s \gamma$. Large parts of the latter can be taken over and used in the NNLL calculation of $B \to X_s \ell^+ \ell^-$. Thanks to the joint effort of several groups [8,9,10,11, 12,13,14,15], the necessary *additional* NNLL calculations have been practically finalized by now.

The computation of all the missing initial conditions to NNLL precision has been presented in Ref. [8]. The most relevant missing piece of the anomalous dimension matrix, namely the three-loop mixing of four-quark operators into semileptonic ones, has been obtained very recently in Ref. [9]. Thanks to these works, the large matching scale uncertainty of around 16% of the NLL prediction has been removed.

The two-loop matrix elements of the four-quark operators are probably the most difficult part of the NNLL enterprise. Asatrian et al. succeeded in using a mass and momentum double expansion of the virtual two-loop diagrams [10]. This calculation is based on expansion techniques which can be applied only in the lower perturbative window of the dilepton spectrum. Once the $c\bar{c}$ threshold is reached, the momentum expansion is not a valid procedure anymore. We have recently extended this calculation to the upper perturbative window above the $c\bar{c}$ threshold [14,15]: in the next section we shall present the first phenomenological outcomes of this analysis. We resorted to semi-numerical methods, which are valid both below and above the threshold. Regarding the lower perturbative window, our analysis provides as an independent confirmation of [10], which is particularly welcome in view of its complexity: below the $c\bar{c}$ threshold the agreement between our results and those of [10] is excellent. As shown in [10], the NNLL matrix element contributions are a fundamental ingredient to reduce the perturbative uncertainty: in the lower window the (low) scale dependence gets reduced from 13% to 6.5%. As we shall discuss in the next section, the residual scale dependence in the upper window is even smaller, around the 3% level.

Another independent ingredient of the NNLL analysis is represented by bremsstrahlung corrections (and corresponding virtual soft-gluon terms). Also this part of the calculation is now available and cross-checked for both dilepton spectrum and FB asymmetry [10,11,12,13]. While the NNLL program for the FB asymmetry is fully completed [12,13], in principle there are some pieces still missing for the integrated dilepton spectrum; however, all of them are estimated to be below 1% at the branching ratio level. Note that, at this level of accuracy, other subleading effects become more important. For instance, further studies regarding higher-order electromagnetic effects should deem necessary.

3 Results

Before discussing the numerical predictions for the integrated branching ratios, it is worth to emphasize that low- and high-dilepton mass regions have complementary virtues and disadvantages. These can be summarized as follows ($q^2 = M^2_{\ell^+\ell^-}$):

Virtues of the low-q^2 region: reliable q^2 spectrum; small $1/m_b$ corrections; sensitivity to the interference of C_7 and C_9; high rate.
Disadvantages of the low-q^2 region: difficult to perform a fully inclusive measurement (severe cuts on the dilepton energy and/or the hadronic invariant mass); long-distance effects due to processes of the type $B \to \Psi X_s \to X_s + X' \ell^+ \ell^-$ not fully under control; non-negligible scale and m_c dependence.

Virtues of the high-q^2 region: negligible scale and m_c dependence due to the strong sensitivity to the Wilson coefficient $|C_{10}|^2$; easier to perform a fully inclusive measurement (small hadronic invariant mass); negligible long-distance effects of the type $B \to \Psi X_s \to X_s + X' \ell^+ \ell^-$.
Disadvantages of the high-q^2 region: q^2 spectrum not reliable; sizable $1/m_b$ corrections; low rate.

Given this situation, we believe that future experiments should try to measure the branching ratios in both regions and report separately the two results. These two measurements are indeed affected by different systematic uncertainties (of theoretical nature) but they provide different short-distance information.

In order to obtain theoretical predictions that can be confronted with experiments, it is necessary to convert the $s = q^2/m_b^2$ range into a range for the measurable dilepton invariant mass q^2. Concerning the low-q^2 region, we propose as reference interval the range $q^2 \in [1, 6]$ GeV^2. The lower bound on q^2 is imposed in order to cut a region where there is no new information with respect to $B \to X_s \gamma$ and where we cannot trivially combine electron and muon modes. Taking into account the input values in Table 1, the NNLL prediction within the SM is:

$$R^{\rm low}_{\rm cut} = \int_{1\ {\rm GeV}^2}^{6\ {\rm GeV}^2} dq^2 \frac{d\Gamma(B \to X_s \ell^+ \ell^-)}{\Gamma(B \to X_c e \nu)} = 1.48 \times 10^{-5}$$

$m_b^{\rm pole} = (4.9 \pm 0.1)$ GeV	$m_c/m_b = 0.29 \pm 0.02$
$\alpha_s(M_Z) = 0.119$	$\alpha_{\rm em} = 1/128$
$\mu = \left(5.0^{+5.0}_{-2.5}\right)$ GeV	$\vert V_{ts}/V_{cb}\vert = 0.97$

Table 1. Main input values used in the numerical analysis.

$$\times \left[1 \pm 8\%\big|_{\Gamma_{\rm sl}} \pm 6.5\%\big|_{\mu} \pm 2\%\big|_{m_c} \pm 3\%\big|_{m_b({\rm cuts})} + (4.5 \pm 2)\%\big|_{1/m_b^2} - (1.5 \pm 3)\%\big|_{c\bar{c}} \right] = (1.52 \pm 0.18) \times 10^{-5} \ . \quad (1)$$

The error denoted by $\Gamma_{\rm sl}$ corresponds to the theoretical uncertainty implied by the $\Gamma(B \to X_c e \nu)$ normalization which, in turn, is dominated by the uncertainty on m_c. As already stressed in Ref. [10], at present this is the dominant source of uncertainty in the low-q^2 region. In principle, alternative normalizations such as the one proposed in Ref. [16] using $B \to X_u \ell \nu$ could be used to reduce this uncertainty in the future; however, in practice this is still the best we can do at the moment. Using the world average $\Gamma(B \to X_c e \nu) = (10.2 \pm 0.4)\%$, we finally obtain:

$$BR(q^2 \in [1,6]\ {\rm GeV}^2) = (1.55 \pm 0.19) \times 10^{-6} \ . \quad (2)$$

Concerning the high-dilepton mass region, we propose as a reference cut $q^2 > 14.4 {\rm GeV}^2$. Using our new NNLL evaluation of the two-loop matrix elements (and reanalyzing nonperturbative effects in this region) we find:

$$R_{\rm cut}^{\rm high} = \int_{q^2 > 14.4\ {\rm GeV}^2} dq^2 \frac{d\Gamma(B \to X_s \ell^+ \ell^-)}{\Gamma(B \to X_c e \nu)} = = 4.09 \times 10^{-6} \times \left[1 \pm 8\%\big|_{\Gamma_{\rm sl}} \pm 3\%\big|_{\mu} \pm 15\%\big|_{m_b({\rm cuts})} - (8 \pm 8)\%\big|_{1/m_b^{(2,3)}} \pm 3\%\big|_{c\bar{c}} \right] = (3.76 \pm 0.72) \times 10^{-6} \ , \quad (3)$$

or

$$BR(q^2 > 14.4\ {\rm GeV}^2) = (3.84 \pm 0.75) \times 10^{-7} \ . \quad (4)$$

As can be noted, in this case μ dependence and intrinsic m_c dependence induce a negligible uncertainty. In addition to the semileptonic normalization (which induces a common uncertainty to low- and high-q^2 regions), here the largest uncertainties are related to the $1/m_b$ expansion. Most of them are parametric, which could be reduced in the future, with the help of more precise data on charged-current semileptonic decays $B \to X_{u,c} \ell \nu$. The leading 15% error denoted by 'm_b(cuts)' indicates the uncertainty in the relation between the physical q^2 interval and the corresponding interval for the variable s of the partonic calculation: this is nothing but the uncertainty in the relation between m_b and the physical hadron mass. The 8% error denoted by $1/m_b^{(2,3)}$ indicates the combined uncertainty due to $1/m_b^2$ and $1/m_b^3$ corrections: these nonperturbative effects induce a divergence in the q^2 spectrum (for $q^2 \to m_b^2$) which cannot be re-absorbed in a shape function distribution [6,17]. This divergence does not prevent us from making reliable predictions for the integrated rate, but it slows down the convergence of the series, which turns out to be an effective expansion in inverse powers of $m_b(1 - \sqrt{s_{\rm max}})$, rather than m_b.[1]

We finally note that in both cases (low- and high-q^2 regions), we have not explicitly indicated the uncertainty due to $\alpha_{\rm em}$ and $\vert V_{ts}/V_{cb}\vert$, which have been fixed to the values in Table 1. In principle, variations of these parameters can be trivially taken into account by appropriate multiplicative factors (they both appear as a squared multiplicative factors in $R_{\rm cut}$). However, we stress that a coherent treatment of higher-order electromagnetic effects — which is beyond the scope of this work — cannot be simply reabsorbed into a redefinition of $\alpha_{\rm em}$.

References

1. T. Hurth, Rev. Mod. Phys. **75** (2003) 1159 [hep-ph/0212304]
2. J. Kaneko *et al.* [BELLE Collaboration], Phys. Rev. Lett. **90** (2003) 021801 [hep-ex/0208029].
3. K. Abe *et al.* [BELLE Collaboration], hep-ex/0107072.
4. B. Aubert *et al.* [BABAR Collaboration], hep-ex/0308016.
5. A. F. Falk, M. Luke and M. J. Savage, Phys. Rev. **D 49** (1994) 3367 [hep-ph/9308288]; A. Ali, G. Hiller, L. T. Handoko and T. Morozumi, Phys. Rev. **D 55** (1997) 4105 [hep-ph/9609449]; G. Buchalla, G. Isidori and S. J. Rey, Nucl. Phys. **B 511** (1998) 594 [hep-ph/9705253];
6. G. Buchalla and G. Isidori, Nucl. Phys. **B 525** (1998) 333 [hep-ph/9801456].
7. M. Misiak, Nucl. Phys. B **393** (1993) 23; A. J. Buras and M. Munz, Phys. Rev. D **52** (1995) 186 [hep-ph/9501281].
8. C. Bobeth, M. Misiak and J. Urban, Nucl. Phys. B **574**, 291 [hep-ph/9910220].
9. P. Gambino, M. Gorbahn and U. Haisch, hep-ph/0306079.
10. H. H. Asatryan, H. M. Asatrian, C. Greub and M. Walker, Phys. Rev. D **65** (2002) 074004 [hep-ph/0109140].
11. H. H. Asatryan, H. M. Asatrian, C. Greub and M. Walker, Phys. Rev. D **66** (2002) 034009 [hep-ph/0204341].
12. A. Ghinculov, T. Hurth, G. Isidori and Y. P. Yao, Nucl. Phys. B **648** (2003) 254 [hep-ph/0208088];
13. H. M. Asatrian, K. Bieri, C. Greub and A. Hovhannisyan, Phys. Rev. D **66** (2002) 094013 [hep-ph/0209006].
14. A. Ghinculov, T. Hurth, G. Isidori and Y. P. Yao, Nucl. Phys. Proc. Suppl. **116** (2003) 284 [hep-ph/0211197].
15. A. Ghinculov, T. Hurth, G. Isidori and Y. P. Yao, CERN-TH/2003-132.
16. P. Gambino and M. Misiak, Nucl. Phys. B **611** (2001) 338 [hep-ph/0104034].
17. C. W. Bauer and C. N. Burrell, Phys. Lett. B **469** (1999) 248 [hep-ph/9907517].

[1] For a more detailed discussion of these results we refer the reader to [15].